

Supporting Information

Fluoride-Free Synthesis of Large-Pore ITQ-27 Aluminosilicate Zeolite with Tunable Composition and Enhanced Methanol-to-Propylene Performance

Yukun Chen,^{†ab} Chao Ma,^{†b} Ke Long,^b Yuanhao Li,^{bc} Shitai Li,^{bc} Wenna Zhang,^{*bc} Xiaona Liu,^{*bc} Peng
Guo,^{bc} and Zhongmin Liu^{abc}

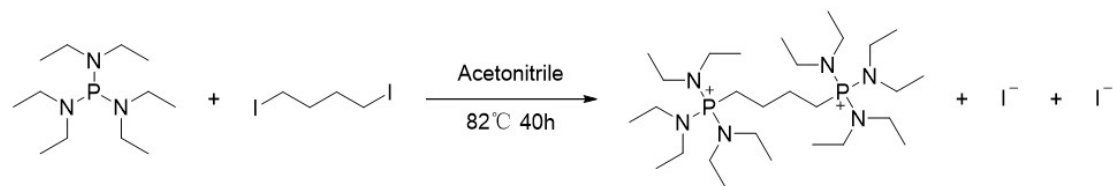
Experimental Section

Ingredients.

Silica gel (LudoxAS40, 40%, Sigma-Aldrich), silver oxide (Ag_2O , 99.7%, Shanghai Aladdin), hydrochloric acid (HCl, 37%, Kermel), tris(diethylamino)phosphine (TDEAP, 97%, Shanghai Aladdin), 1,4-diiodobutane (98%, Shanghai Aladdin), sodium hydroxide solution (NaOH, 35%, Shanghai Aladdin), acetonitrile (99%, Guangdong Guanghua), tert-butyl methyl ether (99%, Sinopharm), aluminum isopropoxide ($\text{Al}(\text{i-PrO})_3$, 98%, Shanghai Aladdin), Deuterium water (99.9%, J&K Scientific).

Preparation of OSDA4.

50 mL anhydrous acetonitrile was added to 250 mL round-bottomed flask containing 50.0 g tri-(diethylamino)phosphine and stirred at room temperature until it became completely transparent. Subsequently, 28.47 g 1,4-diiodobutane was added in batches. Finally, the mixture was refluxed at 82 °C for 40 hours. After reaction, acetonitrile was removed by vacuum rotary evaporation. The obtained product was washed with tert-butyl methyl ether for two times to remove unreacted raw materials. After dried at 60 °C overnight, 69.54 g white solid powder was obtained (94.06% yield). The target phosphonium salt was confirmed by ^{13}C NMR (12.7, 23.6, 24.9, and 39.3 ppm).



The hydroxide form of OSDA4 was obtained by exchanging its iodide form with silver oxide for 4 hours while avoiding exposure to light. The concentrations of OSDA4 hydroxide were determined by titration with 0.1 M hydrochloric acid.

Synthesis of ITQ-27 zeolite.

Zeolite ITQ-27 was synthesized hydrothermally using gel molar compositions of 1 SiO_2 : (0.0665–0.0025) Al_2O_3 : (0–0.05) NaOH: 0.2 OSDA4: (10–30) H_2O . Detailed synthesis conditions are listed in Table S1. The typical synthesis procedure is as follows: $\text{Al}(\text{i-PrO})_3$ was stirred with OSDA4 hydroxide in a Teflon-lined autoclave at room temperature for 1 hour, and a certain amount of aqueous NaOH solution was added if necessary. Then, AS-40 was added and stirred for another 3 hours. Subsequently, excess water was evaporated at 80 °C until target $\text{H}_2\text{O}/\text{SiO}_2$ ratio was achieved. Finally, the autoclave containing synthetic gel was sealed and placed in a static oven at 175 °C. After crystallization, the autoclave was cooled down to room temperature with flowing water. The resulting solid product was separated by centrifugation, washed with deionized water, and dried overnight at 100 °C.

Characterizations.

The crystallinity and phase purity of all samples were determined by PXRD data collected on PANalytical X'Pert PRO X-ray diffractometer with $\text{CuK}\alpha$ radiation ($\lambda=1.5418 \text{ \AA}$) in Bragg-Brentano geometry. Scanning electron microscopy (SEM) images were obtained on a Hitachi SU8020 microscope with accelerating voltage of $2 \times 10^3 \text{ V}$.

Thermogravimetry analysis (TGA) was characterized using a TA Q-600 analyzer with heating rate of 10 °C/min under flowing air condition. The content of Si, Al, and P was determined using PANalytical Axios Advanced X-ray fluorescence spectroscopy (XRF) or Perkin Elmer 7300DV inductively coupled plasma optical emission spectrometer (ICP-OES). N₂ adsorption–desorption measurements were carried out using Micromeritics 3Flex analyzer at 77 K. Before adsorption, calcined ITQ-27 was treated at 623 K for 4 h. The solid-state NMR experiments were conducted using Bruker Avance III 400 spectrometer equipped with 14.1 T wide-bore magnet and 4 mm WVT double-resonance MAS probe. The resonance frequencies of ¹H, ¹³C and ²⁹Si are 600.13, 150.9 and 119.2 MHz, respectively. ¹³C MAS NMR spectra were recorded using cross-polarization (CP, ¹H → ¹³C) sequence with a contact time of 3 ms and a recycle delay of 2 s at spinning rate of 12 kHz. 4096 scans were accumulated to achieve a satisfactory signal-to-noise ratio. Chemical shifts were referenced to adamantane with upfield methine peak at 29.5 ppm. ²⁹Si MAS NMR spectra were recorded with a spinning rate of 8 kHz using high-power proton decoupling. 2048 scans were accumulated with a 60 s recycle delay. Chemical shifts were referenced to kaolinite at -91.5 ppm. ²⁷Al MAS NMR spectra were recorded with a spinning rate of 12 kHz using one pulse sequence, 2048 scans were accumulated with a 2 s recycle delay and a π/8 pulse width of 0.75 ms. Chemical shifts were referenced to (NH₄)Al(SO₄)₂·12H₂O at -0.4 ppm. NH₃-TPD was collected on Micromeritics AutoChem II chemisorption analyser. Before the test, samples were heated to 600 °C and maintained at this temperature for 60 min in the presence of He. Then samples cooled down to 100 °C, adsorbed NH₃ at this temperature for 30 min and purged by He for another 30 min. Finally, samples were heated to 650 °C with a rate of 10 °C/min and TCD was used to detect the signals simultaneously. Infrared spectra of adsorbed pyridine (Py-IR) were recorded on a Thermo Scientific Nicolet iS50 spectrometer equipped with mercury cadmium telluride (MCT) detector. Samples (~5 mg) were pressed into self-supporting wafers and placed in an in-situ cell. Prior to spectral acquisition, the samples were pretreated under N₂ at 573 K for 1 h. After cooling down to 423 K, background spectra were collected in the range of 4000–650 cm⁻¹. Subsequently, pyridine was introduced, and IR spectra were acquired at 423 K after desorbing pyridine at the corresponding temperature for 30 min; spectra were averaged over 32 scans with a resolution of 8 cm⁻¹. Integrated differential phase-contrast scanning transmission electron microscopy (iDPC-STEM) image were performed on FEI Titan Cubed Themis ETEM G3. Three-dimensional electron diffraction (3D ED) data were collected on JEOL 2100 Plus microscope equipped with ASI Cheetah 120 detector.

Density Functional Theory Calculations on Interaction Energies.

The density functional theory (DFT) calculations for geometry optimization were carried out using the Vienna Ab initio Simulation Package (VASP),¹ with the Perdew-Burke-Ernzerhof (PBE) generalized gradient approximated (GGA) exchange-correlation functional.² Grimme-type D3 corrections (DFT-D3) with Becke–Johnson damping were used on dispersion interactions.³ A plane-wave basis was set with a kinetic energy cutoff of 450 eV. Convergence criteria adopted 1.0 × 10⁻⁵ eV for the SCF energy, and 0.05 eV/Å for atomic force, respectively. The unit cell was relaxed during each DFT optimization.

The interaction energy between OSDA and zeolite framework is defined as follows:

$$E_{interaction\ energy} = E_{IWW-OSDA} - E_{IWW} - E_{OSDA}$$

Where:

$E_{interaction\ energy}$ represents the interaction energy between OSDA and zeolite framework

$E_{IWW-OSDA}$ is the energy of the OSDA adsorbed in IWW zeolite framework,

E_{IWW} is the energy of the IWW framework,

E_{OSDA} represents the energy of an isolated OSDA molecule placed in a large box.

Catalytic Reaction.

The synthesized ITQ-27 samples, after being calcined at 600 °C to remove OSDA, can be directly used as catalysts for methanol-to-propylene (MTP) catalytic reaction. MTP reaction was performed in a fixed bed at atmospheric pressure. 100 mg catalyst (40-60 mesh) was transferred to a quartz tubular reactor. Prior to testing MTP activity, catalyst was heated to 550 °C and maintained at this temperature for 30 min in the presence of N₂. Then, the catalyst was cool down to 500 °C naturally. Methanol was fed by passing carrier (32.8 mL/min) gas through a saturator containing methanol at 10 °C, giving weight hourly space velocity (WHSV) of 2 h⁻¹. Furthermore, 33.4 mg catalyst (40-60 mesh) was uniformly mixed with 66.6 mg quartz sand (40-60 mesh), and then filled into the quartz tubular reactor. Under the condition that all other reaction parameters remained unchanged, a WHSV of 6 h⁻¹ was achieved. Agilent 7890B GC equipped with FID detector was used to analyze the products. The conversion and selectivity were calculated on CH₂ basis. Dimethyl ether (DME) was considered as reactant in the calculation.

Tables

Table S1. Detailed synthesis conditions of ITQ-27.

| Run | Gel composition | | | | | Temperature | Time | Phase composition | Si/Al ^a |
|-----|------------------|--------------------------------|--------|------|------------------|-------------|--------|-------------------|--------------------|
| | SiO ₂ | Al ₂ O ₃ | NaOH | OSDA | H ₂ O | | | | |
| 1 | 1 | 0.0665 | - | 0.2 | 10 | 175 °C | 7 d | amorphous | - |
| 2 | 1 | 0.05 | 0.025 | 0.2 | 10 | 175 °C | 10 d | amorphous | - |
| 3 | 1 | 0.05 | 0.05 | 0.2 | 10 | 175 °C | 10 d | amorphous | - |
| 4 | 1 | 0.0335 | - | 0.2 | 10 | 175 °C | 4 d | amorphous | - |
| 5 | 1 | 0.025 | - | 0.2 | 10 | 175 °C | 4.5 d | amorphous | - |
| 6 | 1 | 0.025 | - | 0.2 | 20 | 175 °C | 4 d | amorphous | - |
| 7 | 1 | 0.025 | - | 0.2 | 30 | 175 °C | 4 d | amorphous | - |
| 8 | 1 | 0.025 | - | 0.25 | 10 | 175 °C | 5 d | amorphous | - |
| 9 | 1 | 0.025 | - | 0.3 | 10 | 175 °C | 5 d | amorphous | - |
| 10 | 1 | 0.025 | 0.0125 | 0.2 | 10 | 175 °C | 5 d | amorphous | - |
| 11 | 1 | 0.025 | 0.025 | 0.2 | 10 | 175 °C | 5 d | ITQ-27+amorphous | - |
| 12 | 1 | 0.025 | 0.0375 | 0.2 | 10 | 175 °C | 7.5 d | ITQ-27 | 19 |
| 13 | 1 | 0.025 | 0.0425 | 0.2 | 10 | 175 °C | 7.5 d | ITQ-27 | - |
| 14 | 1 | 0.0165 | - | 0.2 | 10 | 175 °C | 4 d | ITQ-27 | - |
| 15 | 1 | 0.014 | - | 0.2 | 10 | 175 °C | 2.67 d | ITQ-27 | 27.9 |
| 16 | 1 | 0.014 | 0.02 | 0.2 | 10 | 175 °C | 5 d | ITQ-27 | - |
| 17 | 1 | 0.014 | 0.025 | 0.2 | 10 | 175 °C | 5 d | ITQ-27 | - |
| 18 | 1 | 0.014 | 0.03 | 0.2 | 10 | 175 °C | 5 d | ITQ-27 | - |
| 19 | 1 | 0.014 | 0.035 | 0.2 | 10 | 175 °C | 5 d | ITQ-27 | - |
| 20 | 1 | 0.014 | 0.04 | 0.2 | 10 | 175 °C | 5 d | ITQ-27 | - |
| 21 | 1 | 0.014 | 0.045 | 0.2 | 10 | 175 °C | 5 d | ITQ-27 | - |
| 22 | 1 | 0.01 | - | 0.2 | 10 | 175 °C | 5 d | ITQ-27 | 42.9 |
| 23 | 1 | 0.01 | 0.025 | 0.2 | 10 | 175 °C | 4 d | ITQ-27+amorphous | - |

| | | | | | | | | | |
|----|---|--------|-------|-----|----|--------|-----|--------|------|
| 24 | 1 | 0.005 | - | 0.2 | 10 | 175 °C | 5 d | ITQ-27 | 73.0 |
| 25 | 1 | 0.005 | 0.025 | 0.2 | 10 | 175 °C | 5 d | ITQ-27 | - |
| 26 | 1 | 0.0025 | - | 0.2 | 10 | 175 °C | 5 d | ITQ-27 | 83.7 |
| 27 | 1 | 0.0025 | 0.025 | 0.2 | 10 | 175 °C | 5 d | ITQ-27 | - |

[a] The Si/Al ratios of products were calculated based on XRF and ICP results.

Table S2. Textural properties of ITQ-27 catalysts.

| Sample | BET area (m ² g ⁻¹) | t-Plot micropore volume (cm ³ g ⁻¹) |
|--------------|--|--|
| ITQ-27-Run15 | 434.03 | 0.165 |
| ITQ-27-Run22 | 472.50 | 0.172 |
| ITQ-27-Run24 | 529.74 | 0.189 |
| ITQ-27-Run26 | 559.34 | 0.196 |

Table S3. Acid properties of ITQ-27 catalysts.

| Sample | Acid amount (mmol g ⁻¹) ^a | | |
|--------------|--|--------|-------|
| | Weak | Strong | Total |
| ITQ-27-Run15 | 0.282 | 0.073 | 0.355 |
| ITQ-27-Run22 | 0.218 | 0.042 | 0.260 |
| ITQ-27-Run24 | 0.135 | 0.029 | 0.164 |
| ITQ-27-Run26 | 0.135 | 0.028 | 0.163 |

[a] Determined by NH₃-TPD.

Figures

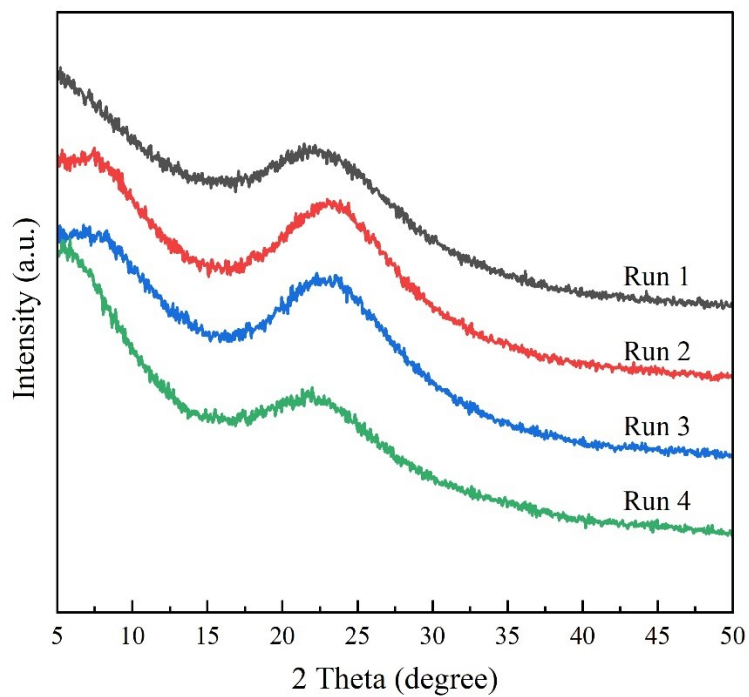


Figure S1. PXRD patterns of Run1-4 products.

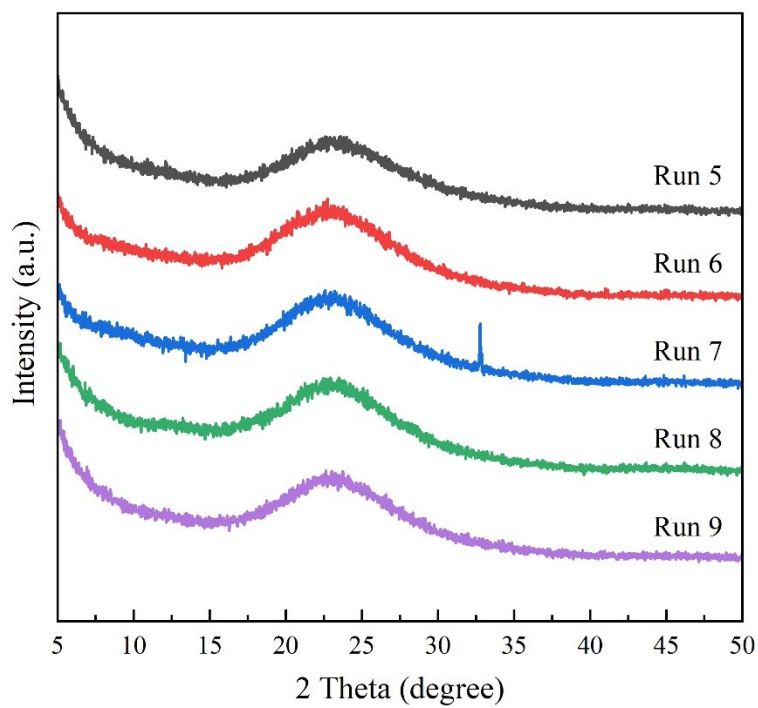


Figure S2. PXRD patterns of Run5-9 products.

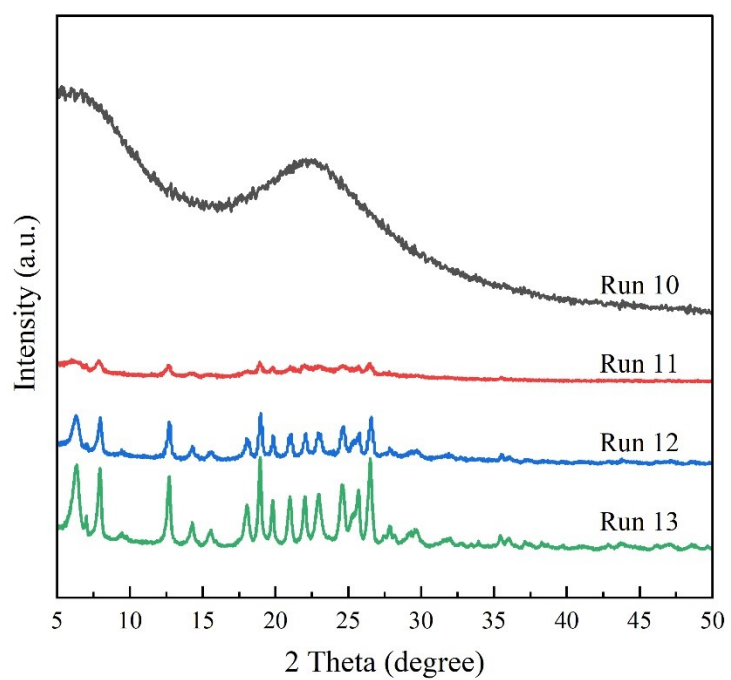


Figure S3. PXRD patterns of Run10-13 products.

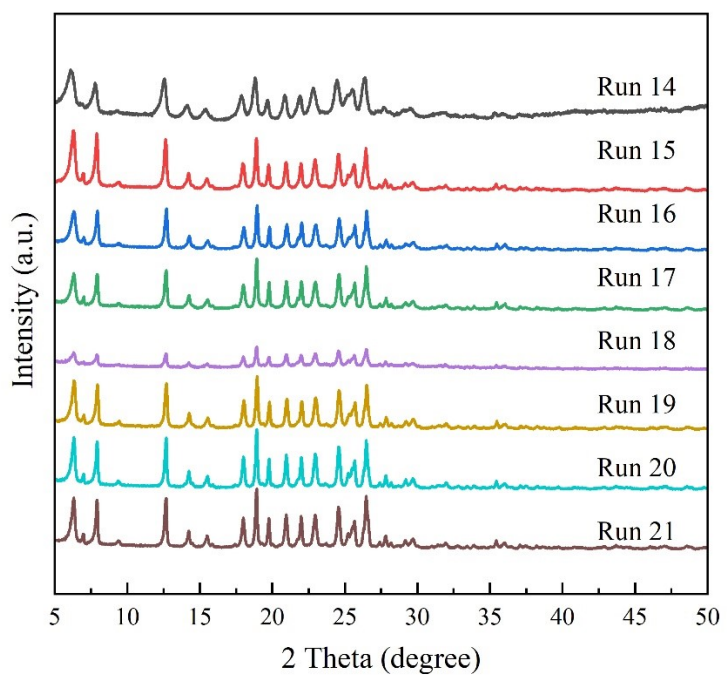


Figure S4. PXRD patterns of Run14-21 products.

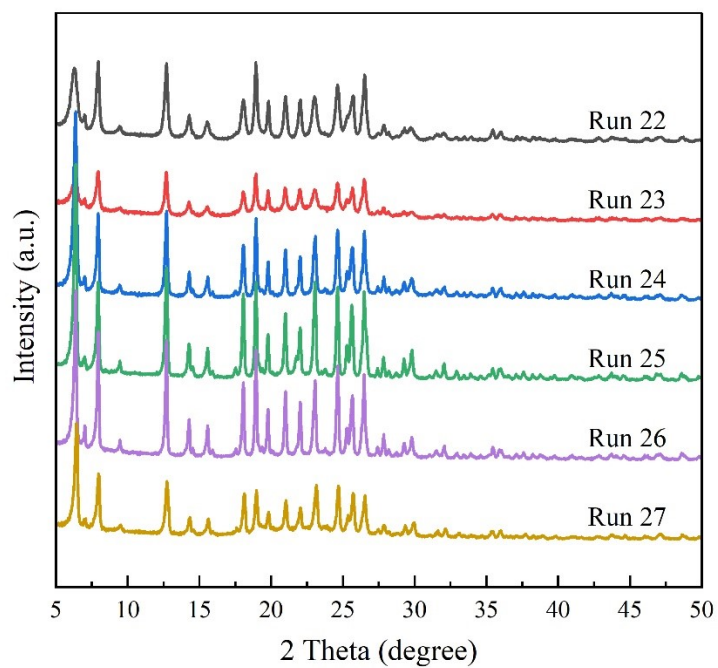


Figure S5. PXRD patterns of Run22-27 products.

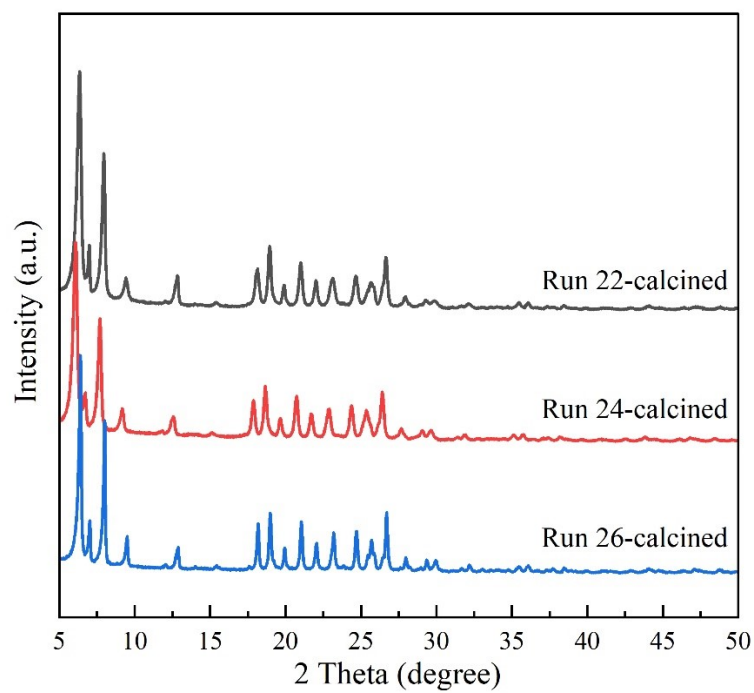


Figure S6. PXRD patterns of calcined ITQ-27-Run22, ITQ-27-Run24, and ITQ-27-Run26.

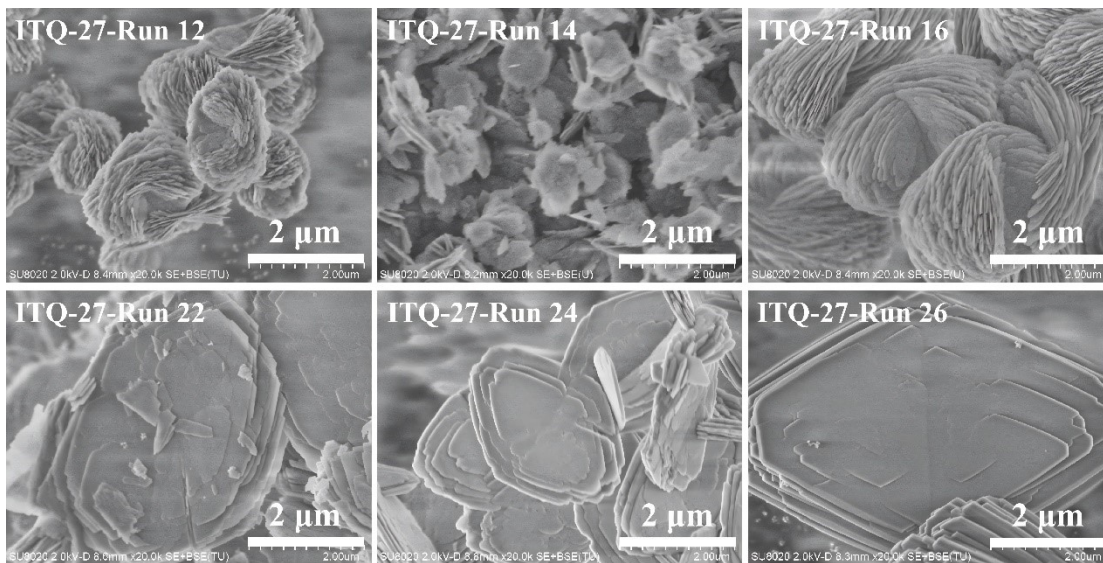


Figure S7. SEM images of synthesized pure-phase ITQ-27 samples.

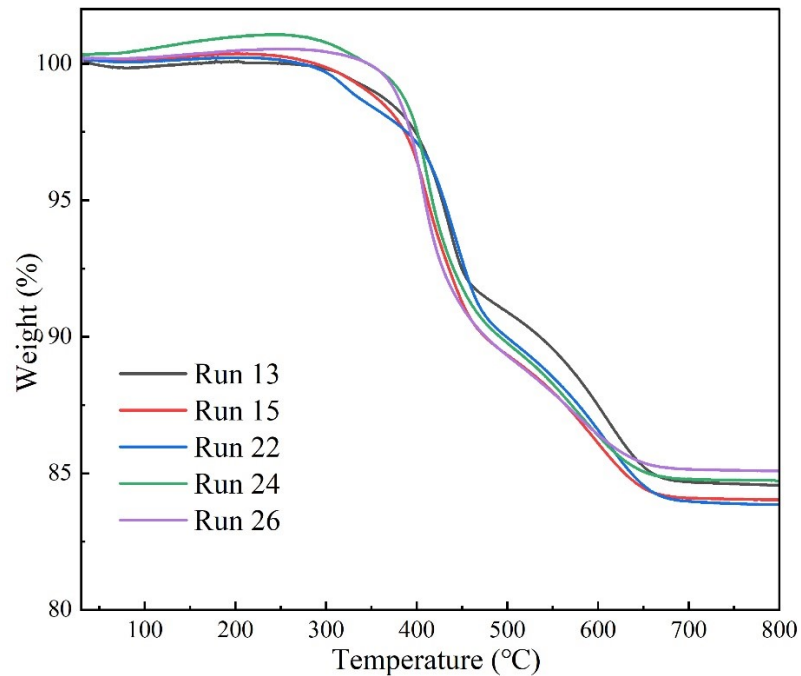


Figure S8. TG isotherms of ITQ-27-Run13, ITQ-27-Run15, ITQ-27-Run22, ITQ-27-Run24, and ITQ-27-Run26.

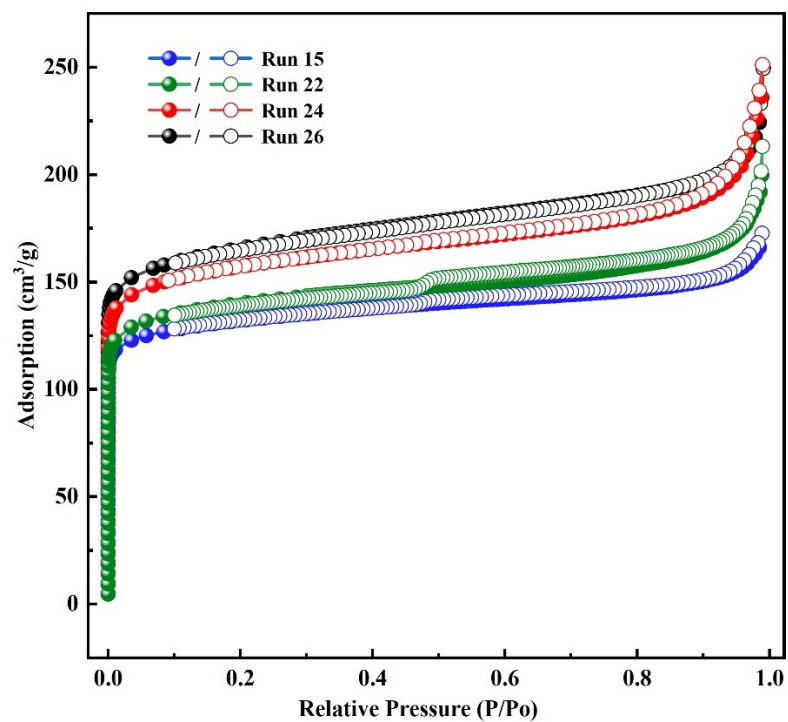


Figure S9. N₂ adsorption-desorption isotherms of ITQ-27-Run15, ITQ-27-Run22, ITQ-27-Run24, and ITQ-27-Run26 collected at 77 K.

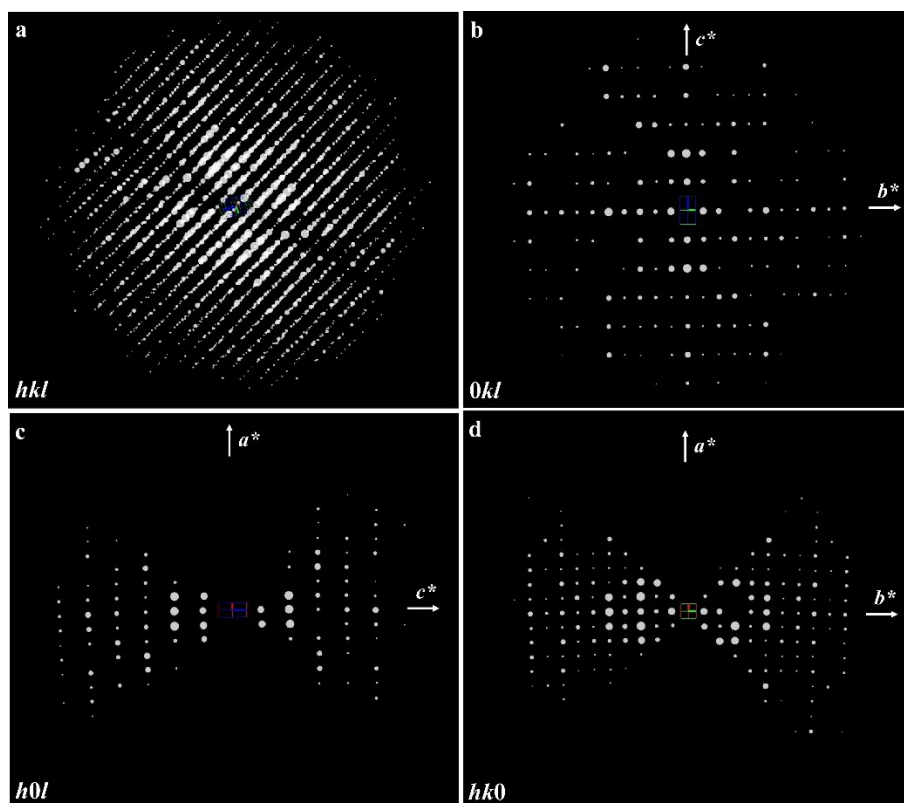


Figure S10. (a) Three-dimensional (3D) reconstructed reciprocal lattice of ITQ-27-Run26. (b-d) Three slices $0kl$, $h0l$, and $hk0$ extracted from the reconstructed reciprocal lattice. Reflection conditions: hkl : $k+k = 2n$, $h+l = 2n$, $h+k = 2n$; $0kl$: $k = 2n$, $l = 2n$; $h0l$: $h = 2n$, $l = 2n$; $hk0$: $h = 2n$, $k = 2n$; $h00$: $h = 2n$; $0k0$: $k = 2n$; $00l$: $l = 2n$.

Note: 273 electron diffraction frames ranging from -61.5° to 57.3° were collected within three minutes. The reconstructed reciprocal lattice can be indexed with an orthorhombic unit cell: $a = 13.8 \text{ \AA}$, $b = 25.1 \text{ \AA}$, $c = 27.6 \text{ \AA}$. According to the reflection conditions, the possible space groups are $F222$, $Fmm2$, and $Fmmm$. Finally, ITQ-27 was successfully solved with $Fmmm$.

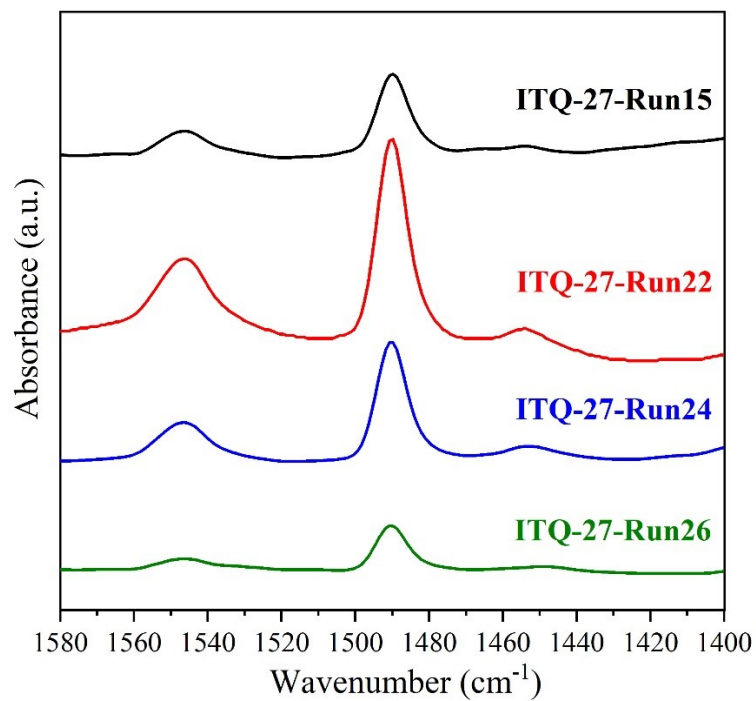


Figure S11. Py-IR spectrum of ITQ-27-Run15, ITQ-27-Run22, ITQ-27-Run24, and ITQ-27-Run26.

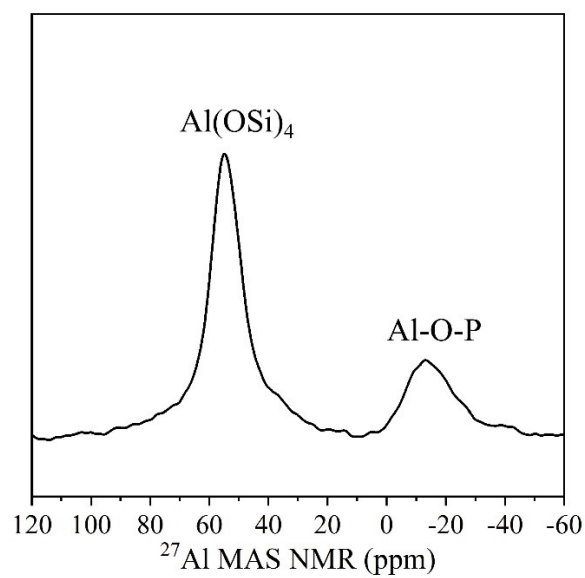


Figure S12. ²⁷Al MAS NMR spectra of ITQ-27-Run22 catalyst.

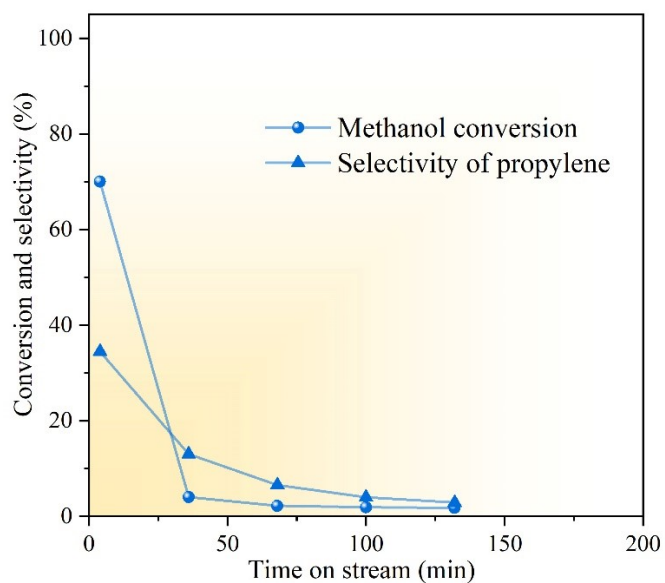


Figure S13. The methanol conversion and propylene selectivity as a function of reaction time over ITQ-27-Run24 catalyst at 500 °C, atmospheric pressure and WHSV of 2 h⁻¹.

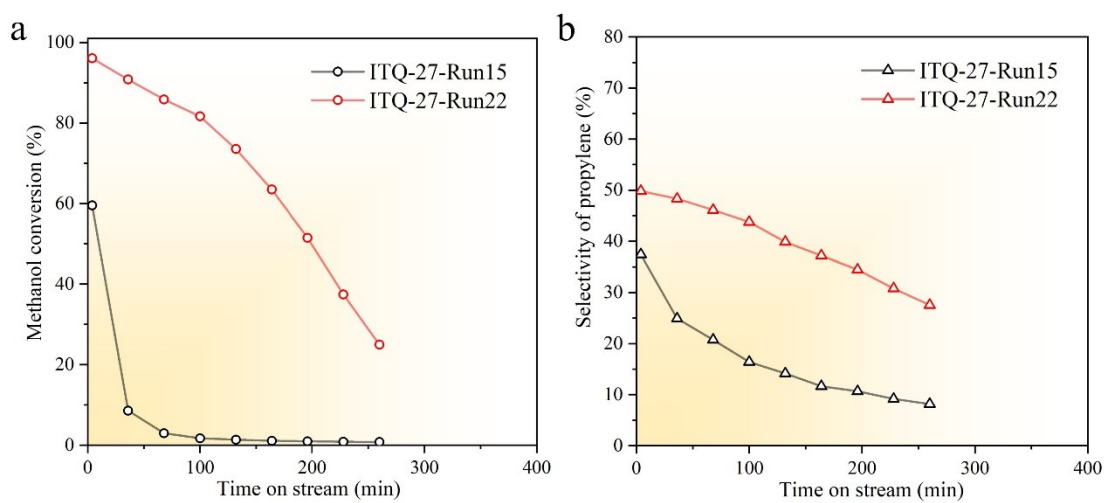


Figure S14. The methanol conversion (a) and propylene selectivity (b) as a function of reaction time over ITQ-27-Run15 and ITQ-27-Run22 at 500 °C, atmospheric pressure and WHSV of 6 h⁻¹.

Reference:

- [1] G. Kresse and J. Furthmüller, *Phys Rev B*, 1996, **54**, 11169–11186.
- [2] J. P. Perdew, K. Burke and M. Ernzerhof, *Phys Rev Lett*, 1996, **77**, 3865–3868.
- [3] S. Grimme, J. Antony, S. Ehrlich and H. Krieg, *J. Chem. Phys.*, 2010, **132**, 154104.